Supporting Information

Effect of Synthesis on Performance of MXene/Iron Oxide Anode Material for Lithium-Ion Batteries

*Adnan Ali[1], Kanit Hantanasirisakul[2], Ahmed Abdala[3], Patrick Urbankowski[2], Meng-Qiang Zhao, Babak Anasori[2], Yury Gogotsi[2], Brahim Aïssa[1], and Khaled A. Mahmoud[1]**

[1]Qatar Environment and Energy Research Institute (QEERI), Hamad Bin Khalifa University, P.O. Box 34110, Doha, Qatar

[2]Department of Materials Science and Engineering and A.J. Drexel Nanomaterials Institute, Drexel University, Philadelphia, PA 19104, USA

[3]Chemical Engineering Program, Texas A&M University at Qatar, POB 23874, Doha, Qatar

Table S1: Atomic wt. % extracted from EDS analysis for BM25.

El	AN	Series	Unn. C [wt. %]	Norm. C [wt. %]	Atom. C [at. %]	Error	(1 Sigma) [wt. %]
O	8	K-series	28.11	32.29	56.74		3.91
Ti	22	K-series	23.24	26.70	15.68		0.93
Fe	26	K-series	31.47	36.15	18.20		1.69
Al	13	K-series	1.34	1.54	1.60		0.11
C	6	K-series	2.90	3.33	7.79		0.70
		Total:	87.05	100.00	100.00		

Table S2. XPS peak fitting of results-shown in **Figure 4**a for Ti_3C_2 and Fe_2O_3 nanoparticles (HT-25). The numbers in parentheses in column 2 are peak locations of Ti $2p_{1/2}$; their full-widths at half maximum, FWHM, are listed in column 3 in parentheses.

Region	BE [eV]	FWHM [eV]	Fraction	Assigned to	Reference
Ti $2p_{3/2}$ ($2p_{1/2}$)	455.2 (461.4)	1.0 (2.1)	0.10	C-Ti-T_x	[1]
	456.3 (461.8)	1.1 (1.9)	0.12	C-Ti^{2+}-T_x	[1]
	457.4 (463.1)	1.2 (1.2)	0.11	C-Ti^{3+}-T_x	[1]
	459.2 (464.8)	1.2 (2.2)	0.50	TiO_2	[1]
	450.0 (466.0)	1.3 (1.7)	0.7	TiO_2-F	[1]
	461.1 (467.1)	1.9 (3.0)	0.10	C-Ti-F	[1]
Fe $2p_{3/2}$ ($2p_{1/2}$)	711.0 (724.7)	3.7 (4.0)	0.81	Fe_2O_3	[2]
	719.5	5	0.11	Fe_2O_3 $2p_{3/2}$ satellite peak	[2]
	733.2	5	0.08	Fe_2O_3 $2p_{1/2}$ satellite peak	[3]

Table S3. XPS peak fitting of results-shown in Figure 4b for Ti_3C_2 and Fe_2O_3 nanoparticles (WS-25). The numbers in parentheses in column 2 are peak locations of Ti 2p1/2; their full-widths at half maximum, FWHM, are listed in column 3 in parentheses.

Region	BE [eV]	FWHM [eV]	Fraction	Assigned to	Reference
Ti $2p_{3/2}$ ($2p_{1/2}$)	455.2 (461.4)	1.0 (2.0)	0.08	C-Ti-T_x	[1]
	456.51 (462.0)	1.6 (1.6)	0.14	C-Ti^{2+}-T_x	[1]
	457.8 (463.5)	0.7 (1.6)	0.02	C-Ti^{3+}-T_x	[1]
	459.3 (464.9)	1.3 (2.2)	0.60	TiO_2	[1]
	459.8 (465.8)	1.2 (2.5)	0.05	TiO_2-F	[1]
	460.7 (466.7)	1.5 (2.0)	0.11	C-Ti-F	[1]
Fe $2p_{3/2}$ ($2p_{1/2}$)	711.0 (724.5)	3.2 (4.4)	0.83	Fe_2O_3	[2]
	718.8	5.0	0.11	Fe_2O_3 $2p_{3/2}$ satellite peak	[2]
	733.6	5.0	0.06	Fe_2O_3 $2p_{1/2}$ satellite peak	[3]

Table S4. XPS peak fitting of results-shown in **Figure 4c** for Ti_3C_2 and Fe_2O_3 nanoparticles (BM-25). The numbers in parentheses in column 2 are peak locations of Ti $2p_{1/2}$; their full-widths at half maximum, FWHM, are listed in column 3 in parentheses.

Region	BE [eV]	FWHM [eV]	Fraction	Assigned to	Reference
Ti $2p_{3/2}$ ($2p_{1/2}$)	455.2 (461.4)	0.9 (1.5)	0.14	C-Ti-T_x	[1]
	456.2 (461.7)	1.6 (1.6)	0.35	C-Ti^{2+}-T_x	[1]
	457.4 (463.1)	1.7 (1.5)	0.21	C-Ti^{3+}-T_x	[1]
	459.1 (464.7)	1.7 (2.0)	0.17	TiO_2	[1]
	459.6 (465.6)	1.6 (2.0)	0.07	TiO_2-F	[1]
	460.7 (466.7)	1.0 (1.7)	0.06	C-Ti-F	[1]
Fe $2p_{3/2}$ ($2p_{1/2}$)	711.4 (724.7)	3.0 (3.8)	0.87	Fe_2O_3	[2]
	719.4	4	0.09	Fe_2O_3 $2p_{3/2}$ satellite peak	[2]
	733.3	5	0.04	Fe_2O_3 $2p_{1/2}$ satellite peak	[3]

Table S5. XPS peak fitting of results-shown in **Figure 4d** for Ti_3C_2 and Fe_2O_3 nanoparticles (BM-50). The numbers in parentheses in column 2 are peak locations of Ti 2p1/2; their full-widths at half maximum, FWHM, are listed in column 3 in parentheses.

Region	BE [eV]	FWHM [eV]	Fraction	Assigned to	Reference
Ti $2p_{3/2}$ ($2p_{1/2}$)	455.1 (461.3)	0.8 (1.4)	0.11	C-Ti-T_x	[1]
	456.0 (461.5)	1.7 (1.7)	0.44	C-Ti^{2+}-T_x	[1]
	457.3 (463.0)	1.3 (1.3)	0.14	C-Ti^{3+}-T_x	[1]
	458.9 (464.6)	1.6 (2.0)	0.18	TiO_2	[1]
	459.4 (465.4)	1.0 (2.0)	0.00	TiO_2-F	[1]
	460.0 (466.0)	1.6 (2.0)	0.13	C-Ti-F	[1]
Fe $2p_{3/2}$ ($2p_{1/2}$)	711.2 (724.6)	2.7 (3.2)	0.94	Fe_2O_3	[2]
	719.3	3.7	0.05	Fe_2O_3 $2p_{3/2}$ satellite peak	[2]
	733.2	1.7	0.01	Fe_2O_3 $2p_{1/2}$ satellite peak	[3]

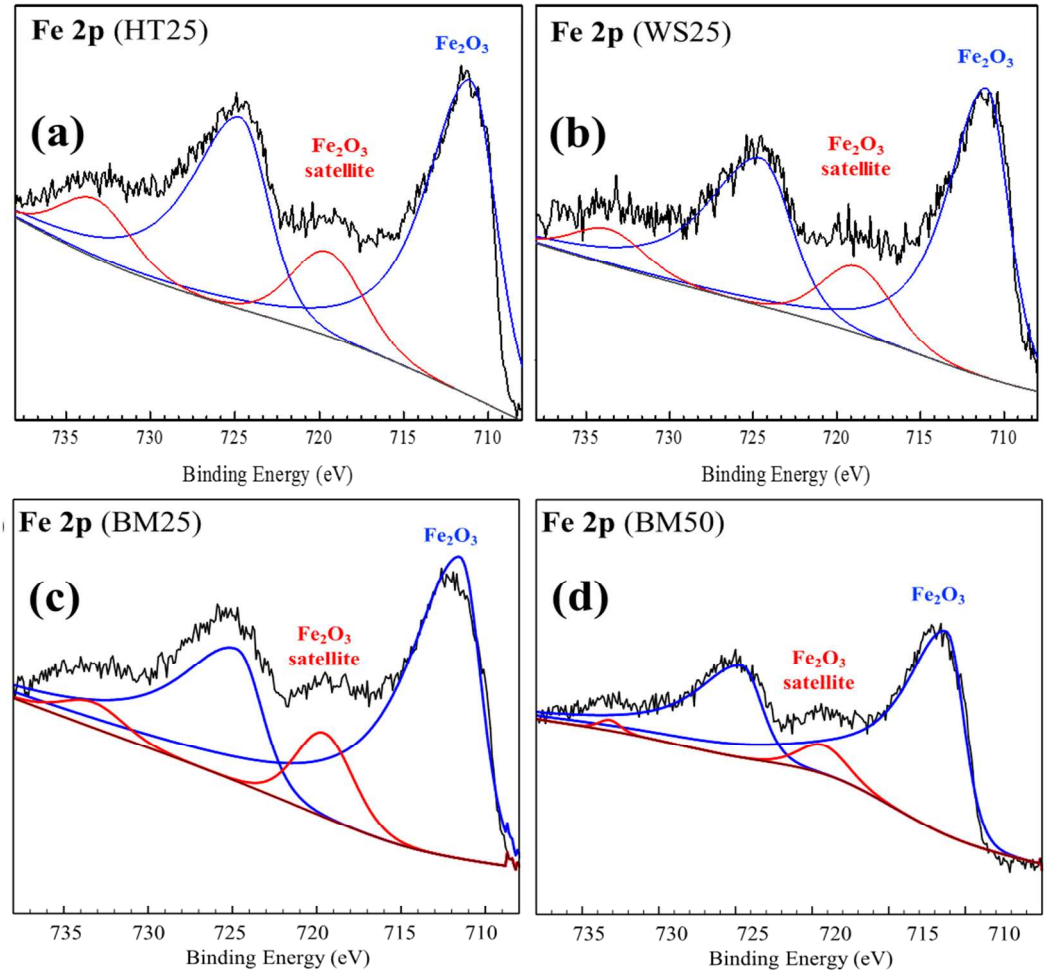

Figure S1. High resolution XPS spectra of Fe2p in $Ti_3C_2T_x/Fe_2O_3$ composites synthesized by a) Hydrothermal (HT25); b) wet sonication (WS25); c) ball milling with 25% Fe_2O_3 (BM25); and d) ball milling with 50% Fe_2O_3 (BM50).[1-3]

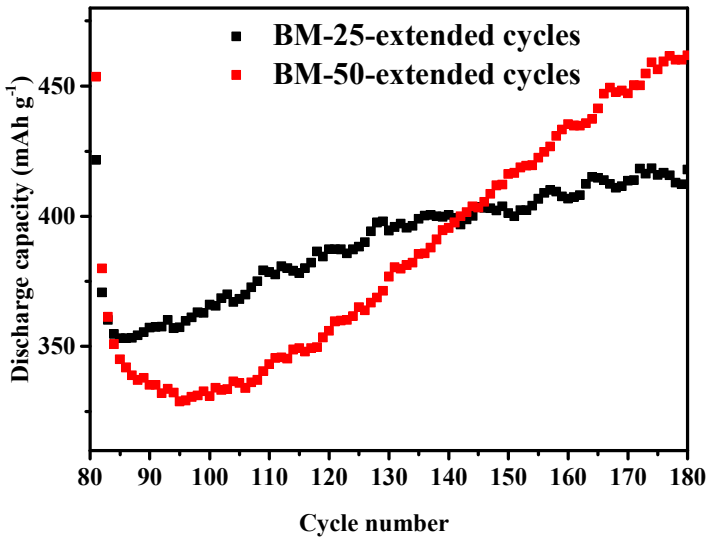

Figure S2. Discharge capacity of composites BM-25 and BM-50 obtained from cycle 80 to 180 at 1 C.

References:

(1) Halim, J.; Cook, K. M.; Naguib, M.; Eklund, P.; Gogotsi, Y.; Rosen, J.; Barsoum, M. W. X-ray photoelectron spectroscopy of select multi-layered transition metal carbides (MXenes). *Applied Surface Science* **2016,** *362*, 406-417, DOI: http://dx.doi.org/10.1016/j.apsusc.2015.11.089.

(2) Nefedov, V. I.; Salyn, Y. V.; Leonhardt, G.; Scheibe, R. A comparison of different spectrometers and charge corrections used in X-ray photoelectron spectroscopy. *Journal of Electron Spectroscopy and Related Phenomena* **1977,** *10* (2), 121-124, DOI: https://doi.org/10.1016/0368-2048(77)85010-X.

(3) Biesinger, M. C.; Payne, B. P.; Grosvenor, A. P.; Lau, L. W. M.; Gerson, A. R.; Smart, R. S. C. Resolving surface chemical states in XPS analysis of first row transition metals, oxides and hydroxides: Cr, Mn, Fe, Co and Ni. *Applied Surface Science* **2011,** *257* (7), 2717-2730, DOI: https://doi.org/10.1016/j.apsusc.2010.10.051.